Received: 20 August 2025 | Revised: 13 October 2025 | Accepted: 18 December 2025 | Published online: 9 January 2026

REVIEW

Journal of Optics and Photonics Research
2026, Vol. 00(00) 1–14
DOI: 10.47852/bonviewJOPR62027286

Advances in Gain Control Techniques for Bismuth-Doped Fiber Amplifier

Lihong Wang[1,2], Ge Wu[1,2], Yidan Zhao[1,2], Jingjing Zheng[1,2*], Li Pei[1,2] and Tigang Ning[1,2]

[1] *Key Lab of All Optical Network & Advanced Telecommunication Network of EMC, Beijing Jiaotong University, China*

[2] *Institute of Lightwave Technology, Beijing Jiaotong University, China*

Abstract: With the explosive growth of global data traffic, extending communication bandwidth is one of the important methods to alleviate the pressure on communication capacity. As the core device of an optical fiber communication system, the bandwidth extension of the optical amplifier is an indispensable research focus. Bismuth-doped fiber amplifier (BDFA) has been widely studied because of its unique broadband luminescence characteristics. In wavelength division multiplexing systems, the signal power fluctuates as the signal goes up and down, and the network is reconstructed. This results in a gain variation of the BDFA, which deteriorates the transmission system performance. The introduction and application of gain control technology can solve this problem well. In addition, the endogenous pump generated by the gain control structure can be combined with the characteristics of bismuth-doped fiber to achieve low-cost and efficient broadband amplification. The combination of these two technologies provides inspiration for the development and application of a broadband amplifier.

Keywords: bismuth-doped fiber, fiber amplifier, gain control

1. Introduction

In recent years, with the rapid development of cloud computing, the Internet of Things, and artificial intelligence technology, the demand for data traffic has increased exponentially. Many examples related to information and communication show that exponential growth can be sustained for decades but eventually saturates [1]. The core challenge of scaling the capacity of optical communication systems in response to the increasing capacity requirements has become a research focus. At present, the main technical approaches include adopting high-order modulation formats, introducing space division multiplexing technology, and widening the available communication band [2–5]. According to Shannon's formula, broadening the bandwidth increases the system capacity linearly. This extension requires the support of the underlying optical communication components.

As a key component of an optical transmission system, the expansion of the operating bandwidth of the optical amplifier is worthy of attention. The silicon-based fiber low-loss window covers 1250–1650 nm. The erbium-doped fiber amplifier (EDFA) operates in the C+L band (1530–1620 nm) [6–10]. Therefore, bismuth-doped fiber amplifier (BDFA) with broadband luminescence in the range of 1150–1800 nm shows great potential in extending the communication bandwidth. The emission bandwidth and emission position of bismuth-doped fiber (BDF) depend on the excitation wavelength and glass composition [11, 12]. By controlling the doping of different elements such as Al, P, Ge, and Si in the glass substrate, the working wavelength of BDFA can be adjusted to fabricate amplifiers applied to different wavelengths [13–18]. Phosphosilicate BDF is often used for amplification in the O band and E band, and its maximum gain has exceeded 40 dB to date [19–21]. A compact O-band BDFA based on the concave cladding fiber structure has been reported [22, 23]. The operating bands of germanium silicate BDF are mainly in the E and S bands [24–26], and wideband amplification in the S+C bands can be achieved by series-connecting erbium-doped fiber (EDF) [27]. The fabrication of U-band amplifiers and lasers can be achieved by highly germanium-doped silicate BDF [13, 28]. The luminescence spectrum of BDF contains multiple emission bands, and the 3 dB bandwidth reaches the range of 200–500 nm [29], which contributes to the bandwidth expansion of fiber amplifiers at the present stage. To date, wideband amplification of BDF in O, E, S, and U bands has been verified.

Not only should parameters such as the bandwidth, gain, and noise figure (NF) of BDFA be considered, but its application within transmission systems also requires attention. Broadband optical amplifiers are typically employed in wavelength division multiplexing (WDM) systems. In WDM communication systems, the change of the sum of optical power values of each channel will lead to transient power fluctuations and low-frequency cross modulation [30]. Usually, the optical amplifier works in the saturation state, and its total output optical power is unchanged. This means that when the number of channels changes, the gain and output power of the remaining channels will change, which worsens the system performance. The gain control technique is an effective way to solve

***Corresponding author:** Jingjing Zheng, Key Lab of All Optical Network & Advanced Telecommunication Network of EMC, Beijing Jiaotong University, and Institute of Lightwave Technology, Beijing Jiaotong University, China. Email: jjzheng@bjtu.edu.cn

these problems. The technique consists of electrical automatic gain control and all-optical automatic gain control. There are three steps to implement electro-automatic gain control: gain detection, signal calibration, and gain regulation. In 1991, Ellis et al. [31] detected part of the amplified signal at the output of EDFA and used the signal to adjust the drive current of the pump to control the gain of EDFA. In 2000, Na et al. [32] proposed to add an additional feedback signal for gain control to the pump. Electrical automatic gain control technology is mature and offers precise control, enabling highly stable output power. It has become the mainstream technology for commercial EDFAs. However, its response speed is limited and constrained by photoelectric conversion. In contrast, all-optical automatic gain control requires a specific wavelength of laser light to be introduced into the amplifier to control the gain. According to the optical feedback structure, all-optical automatic gain control is subdivided into linear cavity gain control [33, 34] and ring cavity gain control [35, 36]. All-optical automatic gain control requires no control circuitry integration, eliminates photoelectric conversion and electronic delays, and avoids electronic bottlenecks. It operates several orders of magnitude faster than electrical automatic gain control and effectively suppresses power transients. However, all-optical control technology remains immature, largely confined to experimental research or preliminary applications, and requires further development.

In particular, gain control technology is one of the key technologies for the application of the new type of broadband fiber amplifier—BDFA in WDM systems. The convergence of these two emerging hotspots has garnered widespread attention and discussion in recent years, serving as a technological reserve to address the challenges of future ultra-high-speed all-optical networks. According to the reported theoretical and experimental research, this paper introduces the basic principle and implementation method of gain control technology, and summarizes the characteristics of several BDFA based on gain control technology, which provides solutions for the application of broadband fiber amplifier in modern optical communication systems.

2. Electrical Automatic Gain Control

Gain control is a key technology used to keep the gain of the fiber amplifier constant, which plays an important role in the stable operation of the optical communication system. According to the component type, the technology is divided into electrical automatic gain control and all-optical automatic gain control. As the name suggests, electrical automatic gain control requires the introduction of feedback circuits to control the gain.

2.1. Electrical automatic gain control method

The principle of electrical automatic gain control is to introduce a feedback circuit to change the pump power according to the change of the output signal power to suppress the gain saturation effect. Figure 1 shows the traditional electric automatic gain control structure. The coupler was used to separate part of the output light into the photodetector to generate an electrical signal, and then the electrical signal was processed by the control circuit acted on the drive current of the pump to realize the regulation of the pump power. In simple terms, as the input signal power changes, the feedback loop adjusts the pump power to keep the gain of the amplifier constant. In 1991, Ellis et al. [31] proposed the basic model of electrical gain control. Moreover, in 2012, Oikawa et al. [37] reported a digitally controlled Automatic gain control EDFA that combines a feed-forward-controlled (FF) pump LD and an FF-controlled variable optical attenuator (VOA) to effectively suppress gain transients, achieving a gain excursion of less than 0.2 dB for a 100-channel equivalent add/drop operation.

2.2. BDFA based on electrical automatic gain control

BDFA has attracted wide attention due to its wideband gain characteristics, but its gain inhomogeneity limits its application in optical communication networks. Combined with the unique performance of BDFA, electrical gain control has a new application. In 2023, Wang et al. [38] explored the relationship between signal wavelength and gain deviation with the help of electrical automatic gain control technology. Figure 2 [38] illustrates the experimental setup. Five laser diodes (LDs) of different wavelengths act as signal sources. The variation of a VOA simulates random light attenuation. Two optical spectrum analyzers receive input and output signals. The automatic gain control system adjusts the pump power to control the amplifier gain according to the collected information. Under automatic gain control, when operating in 1450 ~1490 nm, the gain deviation reduced to ~4%, which is similar magnitude as that in the C-band EDFA. In EDFAs, electronic automatic gain control technology has matured and been commercially deployed. Through the design of electronic feedback loops and optimization of control algorithms, it can achieve high-precision output power stability. However, applying this technology to BDFAs requires switching the operating wavelength band of related components. Replacing and adjusting electro-optic conversion devices within the electronic feedback loop is also complex and costly.

3. All Optical Automatic Gain Control

Electrical gain control has high-precision gain flatness, but the introduction of electronic devices leads to limited response speed [32]. In contrast, the all-optical automatic gain control is composed of optical devices without the intervention of additional control circuits, which has a fast response speed and is conducive to all-optical integration.

3.1. Conventional all-optical automatic gain control method

All-optical automatic gain control requires the introduction of a laser feedback structure in the amplifier to generate a specific

Figure 1
Schematic diagram of electrical automatic gain control

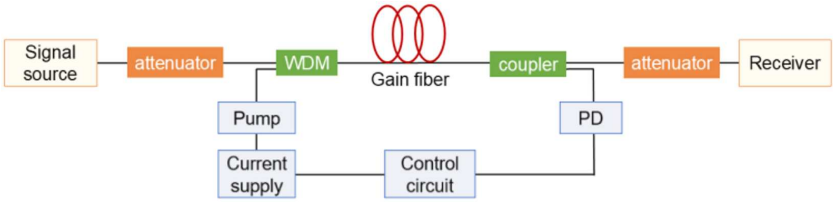

Figure 2
The experimental setup and (b) gain deviation of BDFA with electrical automatic gain control

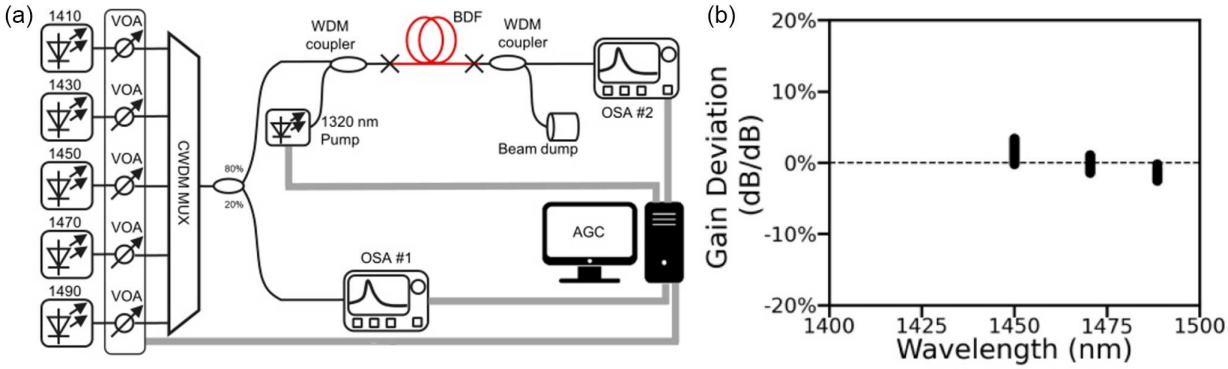

Figure 3
Schematic of (a) linear cavity gain control and (b) annular cavity gain control

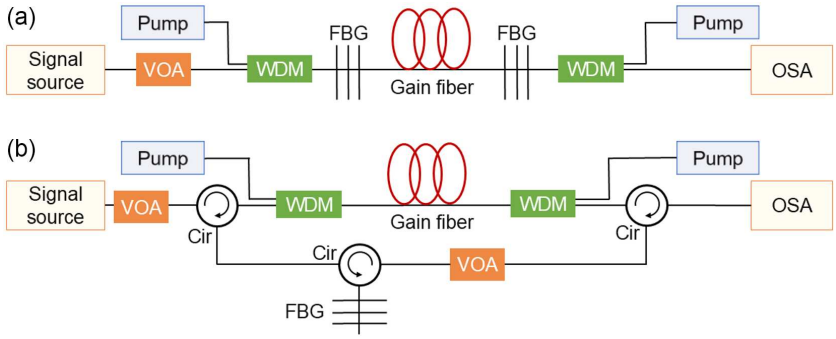

wavelength of control laser and signal to jointly consume the number of inversion particles, to control the gain. According to the type of resonator, all-optical automatic gain control is divided into linear cavity and ring cavity gain control [39–41]. The underlying structures of these two gain controls are presented in Figure 3. Obviously, the structure of the linear cavity is simpler, but the intra-cavity loss of the linear cavity is achieved by replacing the fiber Bragg grating (FBG). The intra-cavity loss of the ring cavity can be realized by directly adjusting the VOA. The change of the loss in the cavity affects the average number of inversion particles to control the gain. According to Yu and Mahony [42], the average number of inversion particles in the gain control case can be expressed as

$$\overline{n} = \frac{\alpha(\lambda_l) + l(\lambda_l)}{\alpha(\lambda_l) + g^*(\lambda_l)} + \frac{-10\log(l_c)/L}{4.34\gamma[\alpha(\lambda_l) + g^*(\lambda_l)]} \tag{1}$$

where λ_l, α, g^*, l, and L represent the laser wavelength, absorption coefficient, emission coefficient, background loss, and gain fiber length, respectively. $l_c$is the effective cavity loss at the control laser wavelength, and $-10\log(l_c)$ is always positive. Depending on the structure, γ is equal to 1 (ring cavity) or 2 (linear cavity). When other things are equal, γ is higher for the linear cavity, and then $\overline{n}$ is smaller. Assuming that the amplifying medium has uniform broadening, the gain of the amplifier at the signal wavelength λ can be expressed as:

$$G(\lambda) = e^{\{[\alpha(\lambda)+g^*(\lambda)]\overline{n} - [\alpha(\lambda)+l(\lambda)]\}L} \tag{2}$$

Therefore, the linear cavity gain control is more efficient for the same intra-cavity loss.

The derivation method described above allows direct testing to determine the number of inverted particles and gain. Of course, another traditional approach involves solving the power transfer equation of the amplifier through numerical analysis to obtain the pump, signal, and amplified spontaneous emission (ASE) powers within the fiber and then calculating the gain and NF. The rate transfer equation for the amplifier is as follows [43]:

$$\frac{\partial N_1}{\partial t} = -W_{12}N_1 + W_{21}N_2 + \frac{N_2}{\tau} \tag{3}$$

$$\frac{\partial N_2}{\partial t} = W_{12}N_1 - W_{21}N_2 - \frac{N_2}{\tau} \tag{4}$$

$$N = N_1 + N_2 \tag{5}$$

where N, N_1, and N_2 denote the total particle number density, ground-state particle number density, and metastable-state particle number density, respectively. τ is the spontaneous emission lifetime. W_{12} and W_{21} represent the ion-stimulated absorption transition rate and stimulated emission transition rate, respectively. We study the amplification process in the steady state, so $\partial N_i/\partial t = 0$. The calculations for W_{12} and W_{21} are as follows:

$$W_{12} = \frac{\Gamma_s\sigma_{12s}P_s\lambda_s}{hcA_{eff}} + \frac{\Gamma_p\sigma_{12p}P_p\lambda_p}{hcA_{eff}} + \frac{\Gamma_s\sigma_{12ase}P_{ase}\lambda_s}{hcA_{eff}} \tag{6}$$

$$W_{21} = \frac{\Gamma_s\sigma_{21s}P_s\lambda_s}{hcA_{eff}} + \frac{\Gamma_p\sigma_{21p}P_p\lambda_p}{hcA_{eff}} + \frac{\Gamma_s\sigma_{21ase}P_{ase}\lambda_s}{hcA_{eff}} \tag{7}$$

where σ_{12s}, σ_{21s}, σ_{12p}, σ_{21p}, σ_{12ase}, and σ_{21ase} represent the signal wavelength absorption cross section, signal wavelength emission cross section, pump wavelength absorption cross section, pump wavelength emission cross section, ASE absorption cross section, and ASE emission cross section, respectively. Γ_s, Γ_p, and Γ_{ase} represent the overlap factors for the signal, pump, and ASE, respectively. λ_s, λ_p, and λ_{ase} denote the wavelengths of the signal, pump, and ASE. h and c are Planck's constant and the speed of light, respectively. A_{eff} is the effective mode field area.

The power variations of the pump, signal, and ASE spectral components within the gain fiber can be described by the power transfer equation:

$$\frac{\partial P_s^{\pm}}{\partial t} = P_s^{\pm}\Gamma_s\left(\sigma_{21s}N_2 - \sigma_{12s}N_1\right) - \alpha_s P_s^{\pm} \tag{8}$$

$$\frac{\partial P_p^{\pm}}{\partial t} = P_p^{\pm}\Gamma_p\left(\sigma_{21p}N_2 - \sigma_{12p}N_1\right) - \alpha_p P_p^{\pm} \tag{9}$$

$$\frac{\partial P_{ase}^{\pm}}{\partial t} = P_{ase}^{\pm}\Gamma_s\left(\sigma_{21ase}N_2 - \sigma_{12ase}N_1\right) - \alpha_s P_{ase}^{\pm} + \frac{2hc^2\Gamma_s\sigma_{21ase}N_2\Delta\lambda}{\lambda^3} \tag{10}$$

where $P_s^{\pm}$, $P_p^{\pm}$, and $P_{ase}^{\pm}$ represent the forward and reverse propagation signals, pump power, and ASE power, respectively. α_s and α_p denote the loss coefficients of the gain fiber at the signal and pump wavelengths.

In Figure 4 [44], we conducted numerical modeling and simulation of the gain control effects of linear cavity and annular cavity amplifiers based on the Matlab platform. In contrast to conventional amplifiers, the boundary conditions of gain control amplifiers need to be adjusted. For the line-cavity gain control amplifier, the boundary conditions are $P_c^+|_{z=0} = R_1 P_c^-|_{z=0}$ and $P_c^-|_{z=L} = \alpha_{VOA}R_2P_c^+|_{z=L}$. P_c^+ and P_c^- represent forward and backward transmission optical power. $z = 0$ and $z = L$ represent the signal input and output positions. R_1, R_2, and α_{VOA} represent the reflectance and intra-cavity loss of the two FBGs. The boundary condition of the loop cavity gain control amplifier is given by $P_c^-|_{z=L} = \alpha_{VOA}P_c^-|_{z=0}$. Based on numerical simulations using MATLAB to solve the rate and power transfer equations, we can directly observe the relationship between gain and input signal power for different gain-clamping techniques, as shown in Figure 4. Under identical VOA losses, the linear cavity gain maintains gain fluctuations below 1 dB across a broader input signal power range, validating the conclusion that the linear cavity gain control structure is more efficient for the same intra-cavity loss.

Figure 4
Theoretical analysis result of ring cavity and linear cavity gain control

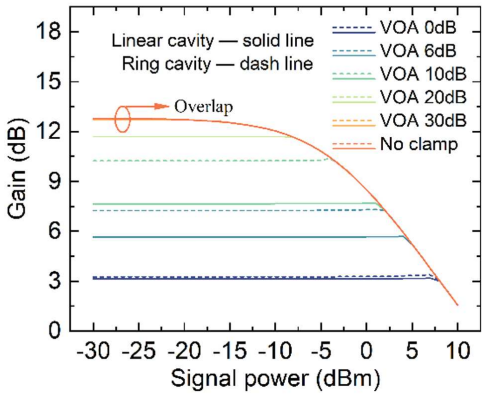

3.2. EDFA based on all-optical automatic gain control

Starting from the traditional linear cavity and annular cavity gain control structures, the research focus has gradually shifted to the structural improvement and performance optimization of EDFA. On this basis, a large number of improvement schemes and research on the gain control structure of EDFA have been reported.

In Luo et al. [45], the control laser clamped part of the gain at 1532 nm, but the gain was not completely clamped at 1552.3 nm due to the inhomogeneous broadening characteristics of EDF. When the number of input channels is changed, the gain depth at 1552.3 nm is changed, resulting in a steady shift of the channel gain. This suggests that gain clamping can only be locally effective in an inhomogeneously broadened medium. Therefore, it is necessary to introduce multi-wavelength control lasers into the gain control structure. In order to suppress the gain transient and steady-state error caused by spectral hole-burning and relaxation oscillation simultaneously, a dual-wavelength all-optical automatic gain control scheme is presented in Figure 5 [46]. Using an F-P filter and two tunable long-period gratings, two control lasers of 1530.5 nm and 1557.2 nm are simultaneously generated in the same loop. The gain change caused by the input power change is less than 0.3 dB under the dual-laser control, while it is 0.8 dB under the single-laser control.

As an amplifier that has been widely applied in optical communication systems, the gain control-related work of EDFA has been widely discussed for a long time. Moreover, this series of work provides an important reference for the subsequent development of BDFA. In 2006, Yi et al. [34] proposed an EDFA with adjustable gain control in a double-pass linear cavity. It has solved the problem of cumbersome operation in adjusting the gain control of traditional linear cavities. Its structure is shown in Figure 6 [34]. The signal is separated from the control laser by using a thin-film filter, and the independent control of the laser power is achieved by adjusting the VOA. The dual-pass configuration involving the circulator is used to enhance the gain.

For the extended band of C-band, that is, L-band, the combination of the multi-stage EDFA scheme and the ring cavity gain control technique achieves high gain, low noise, and gain control [47–49]. Figure 7 [47] shows the scheme and gain-clamping effect of the three-stage ring cavity gain control EDFA. The first-stage EDFA is used as a preamplifier to improve the NF performance. The backward ASE of the C-band enters the ring cavity to achieve gain control. At the same time, the introduction of C-band ASE is beneficial to the gain of L-band. In Liu et al. [8] and Lin et al. [47], the gain of EDFA at 1580 nm is 21.75 dB, the dynamic gain control state is -10 dBm, and the gain change is less than 0.22 dB. The NF is less than 5.5 dB in the range of 1570–1610 nm. In Wu et al. [48], erbium–ytterbium co-doped fiber was used for secondary amplification, with an EDFA gain of 23.78 dB, a dynamic gain control state of -10 dBm, and a gain change of less than 0.09 dB.

The gain control structure is not only applied to single-wavelength gain control but also suitable for flattening the gain spectrum [50–52]. In 2016, Yang et al. [50] investigated a two-stage amplification EDFA based on linear cavity gain control to achieve precise control and flattening of L-band gain. Moreover,

Figure 5
(a) The scheme and (b) dependence of the gain on the signal power for the ring cavity gain control EDFA of the dual-wavelength controlled laser

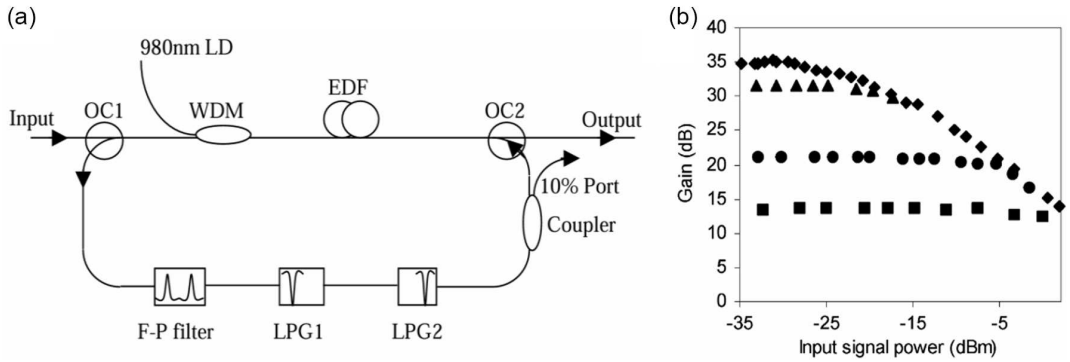

Figure 6
(a) The scheme and (b) dependence of gain on signal power of adjustable linear cavity gain control EDFA

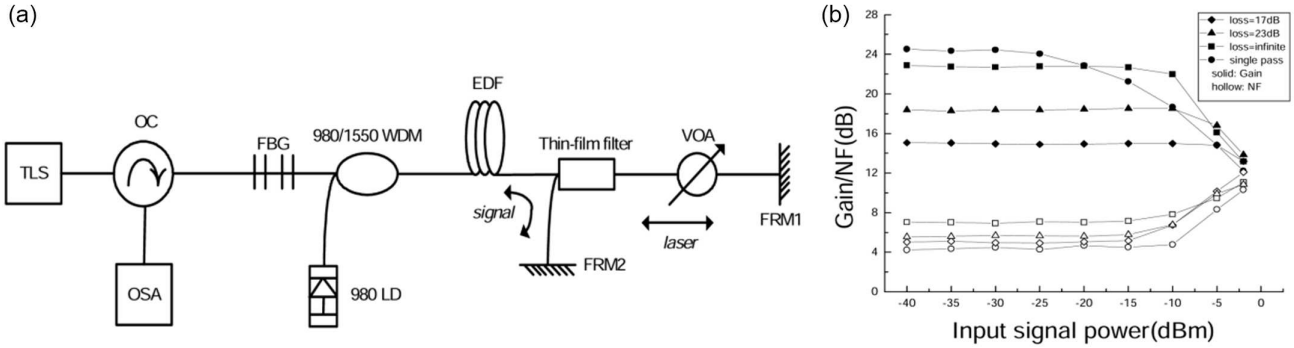

Figure 7
(a) The scheme and (b) gain-clamping effect of three-stage ring cavity gain control EDFA

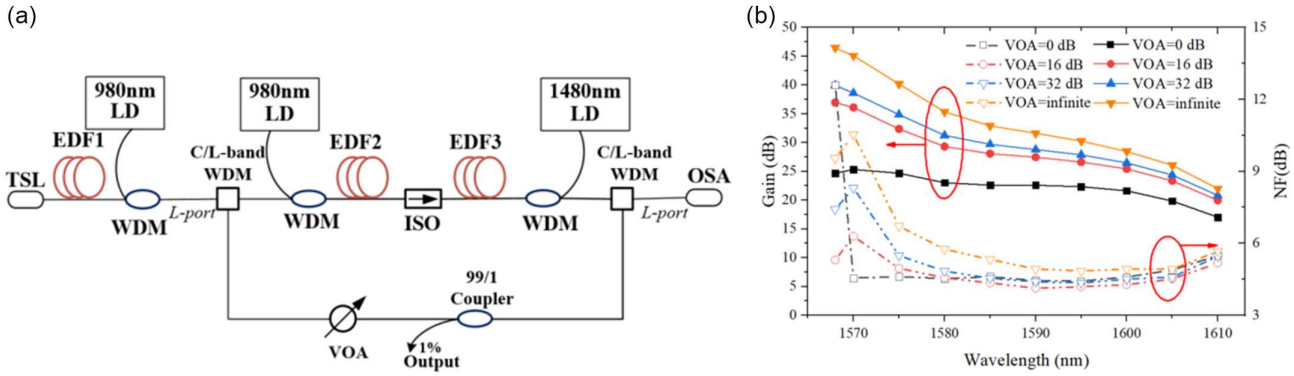

the structure and gain-clamping effect of this EDFA are shown in Figure 8 [50]. In the range of 1570–1610 nm, the gain is 20.2 ± 0.44 dB. The gain fluctuates by 0.1 dB within the signal range of less than -10 dBm. The final structure determined by this scheme is simple, but compared with the scheme shown in Figure 6, it undoubtedly requires more time and effort to replace the FBG during the debugging process. In 2017, the team proposed a novel linear cavity gain-clamped amplifier, in which the resonant cavity is formed by a high-reflectivity uniform FBG and a low-reflectivity chirped FBG. By finely tuning the central wavelength of the uniform FBG, a high-gain output of 24±0.8 dB across the entire L-band was achieved [53].

In 2024, Zhang et al. [54] proposed a tunable linear cavity gain-clamping EDFA. The amplifier employs a two-stage amplification structure, with a gain-clamping configuration based on fiber reflective mirrors and a VOA introduced in the second stage, as shown in Figure 9(a) [54]. The results demonstrate that at 1605 nm, the maximum gain reached 30.5 dB, the minimum NF was 4.8 dB, the dynamic range was 30 dB, and the instability was only 0.1 dB [54]. Compared with conventional linear cavity gain-clamping amplifiers, the broadband reflection of the mirror induces laser mode competition, causing the winning laser to consume more population inversion and effectively compress the signal gain. Meanwhile, the introduction of the VOA not only preserves the

Figure 8
(a) The scheme and (b) gain-clamping effect of linear cavity gain control EDFA controls L-band gain flattening

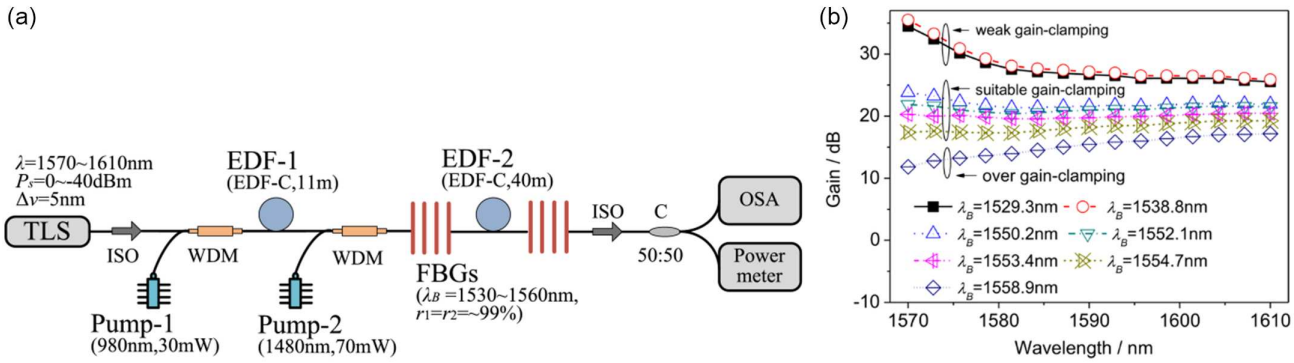

Figure 9
(a) The scheme and (b) dependence of gain on signal power of tunable linear cavity gain control EDFA

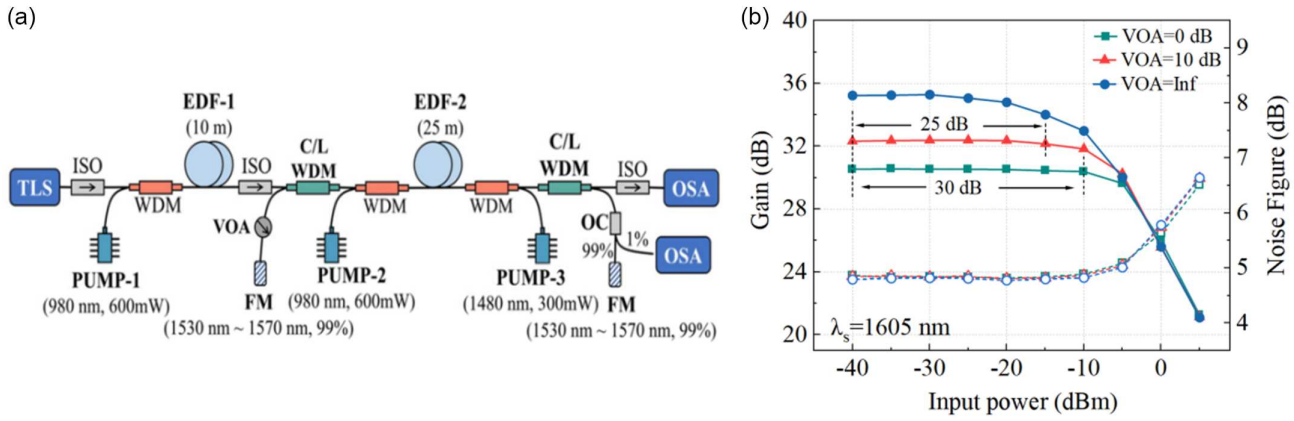

Figure 10
(a) The scheme and (b) dependence of gain on pump power of ring cavity 4-LP-mode gain-clamped EDFA

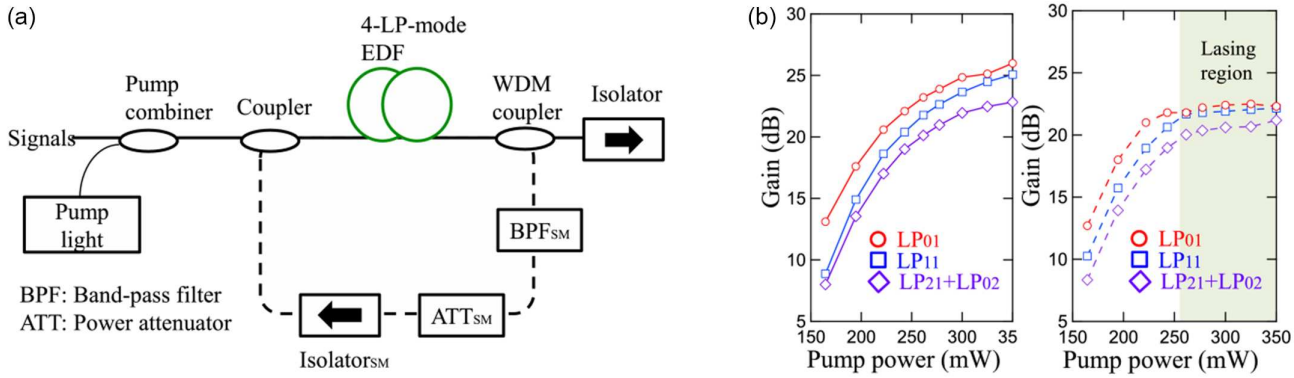

advantages of the linear cavity but also enhances the flexibility of the gain-clamping structure. This study provides a reliable approach and method for the design of gain-clamping amplifiers.

With the development of mode division multiplexing, the related gain control EDFA is worth discussing. In 2018, Wada et al. [55] experimentally evaluated the modal gain characteristics of 4-LP-mode EDFA with gain control and verified that gain-controlled EDFA can simultaneously reduce the temporal modal gain variation in all modes. The scheme and dependence of gain on pump power of the ring cavity 4-LP-mode gain-clamped EDFA are shown in Figure 10 [55]. The application of gain control technology enhances the performance of mode division multiplexing networks and is a promising solution for future optical communication systems.

In 2023, Ono and Yamada [56] investigated the gain controllability of 4-LP-mode EDFAs using both an analytical model and a full model. Through a combination of theoretical and simulation analysis, they demonstrated that for specially designed ring-core fibers, a simple pump power adjustment strategy is sufficient to control the gain error within 0.25 dB. This study provides a new approach to simplifying gain control schemes.

3.3. Bismuth-doped fiber

Unlike EDFA, which relies on gain amplification achieved through the explicit Er^{3+} ion 4f energy level transition [38], BDFA's near-infrared light source originates from different bismuth active centers (BACs) formed within the glass composition. The external electrons of Bi exhibit pronounced matrix dependence in their absorption and emission characteristics due to interactions with different substrate glasses. By doping the main matrix with elements such as Al, P, and Ge, ultra-broadband fluorescence emission spanning 1100–1700 nm can be generated under corresponding pump source excitation. BDFs with different substrates exhibit characteristic luminescent centers. As shown in Figure 11 [29], the luminescent center of bismuth-doped aluminosilicate fiber is located at 1150 nm, phosphosilicate BDF at 1300 nm, while germanosilicate and high-germanium-doped germanosilicate fibers exhibit emission centers at 1450 nm and 1700 nm, respectively [29]. Therefore, selecting different matrix materials and corresponding pump wavelengths enables the creation of BDFAs with distinct gain bands, meeting the demand for broadband gain across various application scenarios.

Figure 12 [57] shows the gain spectra of phosphosilicate and germanosilicate BDFs. Bismuth-doped phosphosilicate fiber has the strongest inhomogeneous broadening among all BDFs. Under different pump wavelengths, BDFA exhibits different emission ranges. As the pump wavelength increases, the gain spectrum of BDFA shifts toward longer wavelengths. For phosphosilicate BDF, when excited with a 1180 nm pump, the gain center is around 1290 nm. If a 1270 nm single-wavelength pump or a combination of 1180 nm and 1270 nm pumps is adopted, the gain center will shift to around 1340 nm, and the gain bandwidth will increase. Long-wavelength gain can be achieved by exciting germanosilicate BDF with a 1270 nm pump, while the gain center will shift to near 1425 nm. Therefore, multi-wavelength pumping and the series connection of BDFs with different doping can further expand the operating bandwidth of BDFA.

Figure 11
Primary pumping wavelengths and emission bands of BDF on different glass substrates

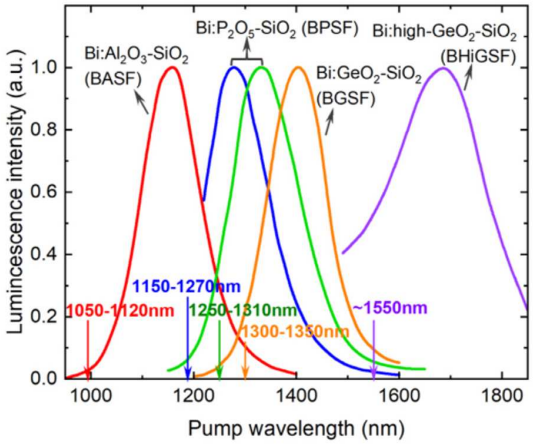

Figure 12
Gain spectra of phosphosilicate BDF and germanium silicate BDF

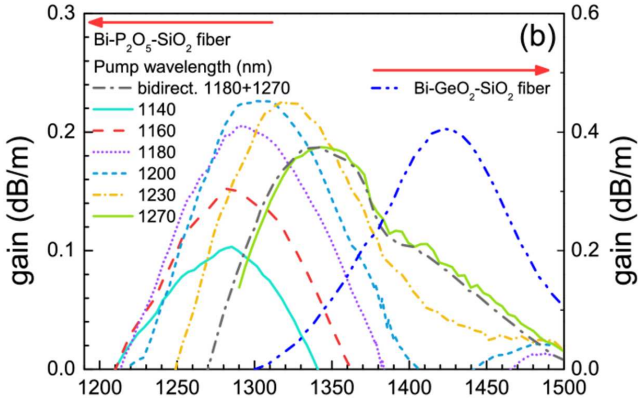

3.4. BDFA based on all-optical automatic gain control

In recent years, BDFA operating in different bands has been realized, and its amplification effect has been getting better. The application and research of related gain control technology have also become a hot topic. Although the pilot research on EDFA has provided support for gain control BDFA, the specific implementation plan still needs to be developed in combination with the characteristics of BDFA.

The gain characteristics of BDFA are significantly affected by inhomogeneous broadening, which is closely related to the diversity of BACs and the inhomogeneity of the glass substrate. Inhomogeneous broadening may lead to spectral hole burning, where gain at specific wavelengths is locally depleted under strong signals or control lasers, forming "depressions" in the gain spectrum. This phenomenon may induce nonlinear crosstalk and gain skew in WDM systems, compromising the uniformity of multi-channel transmission. Therefore, when designing and optimizing gain-clamping structures, it is essential to account for the influence of control laser wavelength on the gain spectrum to prevent gain skew caused by localized population depletion.

3.4.1. All-optical automatic gain control structure achieves BDFA gain stabilization

Electrical automatic gain control, which relies on photodetectors, electronic circuits, and control algorithms, faces challenges including high system upgrade costs and limited response speed. In contrast, all-optical automatic gain control eliminates optoelectronic conversions and electronic processing delays, thereby simplifying the system architecture and avoiding electronic bottlenecks. Its superior response speed also makes it a promising solution for future high-speed, dynamic application scenarios, such as transparent optical networks and optical packet switching, advancing the realization of comprehensive all-optical networks.

1) Tunable ring cavity for gain clamping

In BDFA, the gain stabilization effect of gain control technology can also be realized under different gain-clamping structures. Considering that the ring cavity gain-clamping structure is equipped with VOA to regulate and control the feedback power, research and discussion on the performance of the ring cavity gain-clamping BDFA were conducted in 2024 by Wang et al. [58]. The scheme and dependence of gain on signal power of ring cavity gain-clamped BDFA are shown in Figure 13 [58]. Compared with the conventional amplifier structure, the BDFA with a ring cavity gain-clamping structure achieves gain stability over a wider range of input signals. With a pump power of 500 mW and a VOA loss of 0 dB, the gain variation of the signal less than 6 dBm is less than 0.52 dB, and the average output gain is 6.28 dB. When the

Figure 13
The (a) scheme and (b) dependence of gain on signal power of ring cavity gain-clamped BDFA

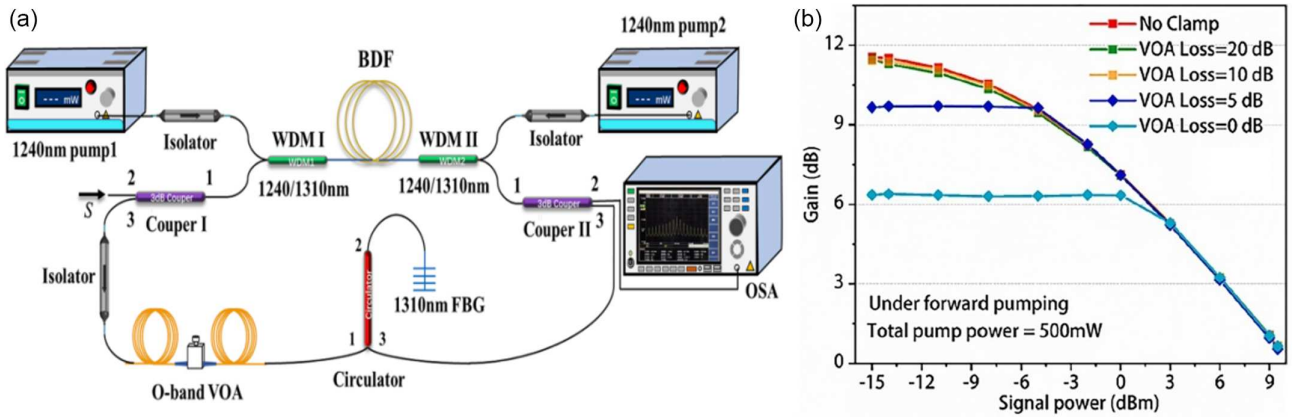

Figure 14
The (a) scheme and (b) gain-clamped operation of BDFA with adjustable semi-ring semi-linear cavity

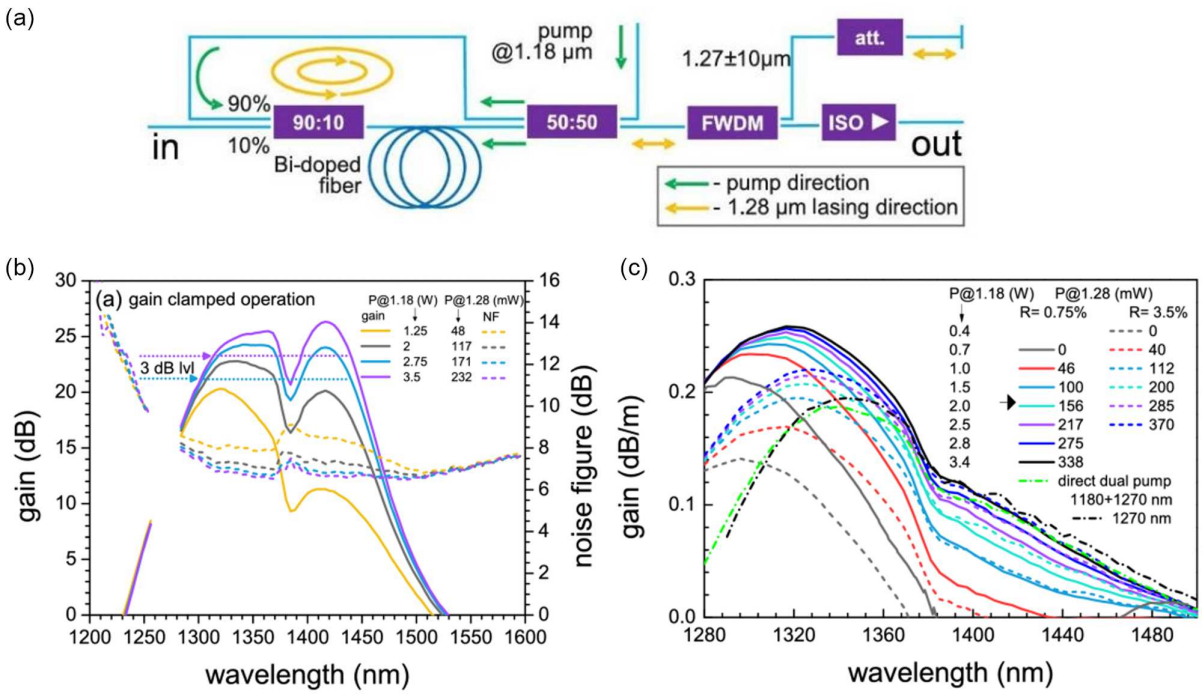

VOA loss is 10 dB, the gain variation of the signal below -2 dBm is less than 3.08 dB, and the average output gain is 13.81 dB.

2) Tunable semi-ring semi-linear cavity for gain clamping

In 2022, Khegai et al. [57] presented their gain-clamped BDFA to investigate the amplifier performance with one- and two-wavelength pumping and gain-clamped schemes. Through the gain control structure, a 1280 nm control laser is generated within the amplifier and acts in conjunction with a 1180 nm pump on the BDF. Compared with the dual-wavelength pump without gain control, the gain coefficient of the BDFA with gain control increases, and the 3 dB bandwidth also increases. Additionally, as observed in Figure 14(b) [57], the power of the 1280 nm control laser increases with the rise in 1180 nm pump power when the external pump power changes. When the control laser power increases, the amplifier gain—particularly at longer wavelengths—also increases. Consequently, the output power rises while the input signal remains unchanged. From Figure 14(c), it is found that when the external pump power at 1180 nm is constant, the increase in reflectance leads to an increase in the control laser power. In this case, the short-wavelength gain decreases and the long-wavelength gain increases. This side shows that different luminescence centers will have obvious differences in their behavior under the action of the same control laser.

This gain-clamped structure generates adjustable feedback power in its linear part, which is similar to that in Yi et al. [34], while the ring cavity part guarantees a much wider path for the feedback power. This structure combines the features of both ring cavity and linear cavity gain-clamping structures, which is why we call it a semi-ring semi-linear cavity for gain clamping.

Figure 15
(a) The scheme and (b) dependence of gain on signal power of tunable gain-clamping linear cavity BDFA with two three-port circulators

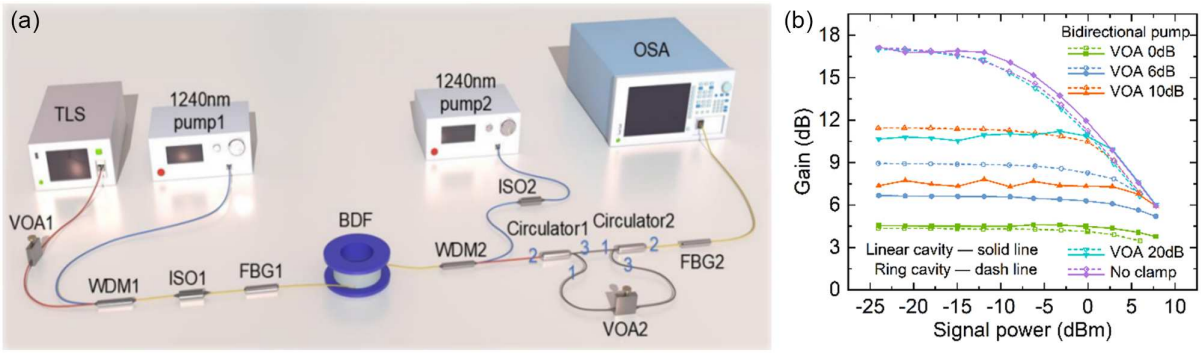

Figure 16
(a) The scheme and (b) dependence of gain on signal power of tunable gain-clamping linear cavity BDFA with a uniform FBG and a triangular FBG (inset: reflection spectrum of the triangular FBG)

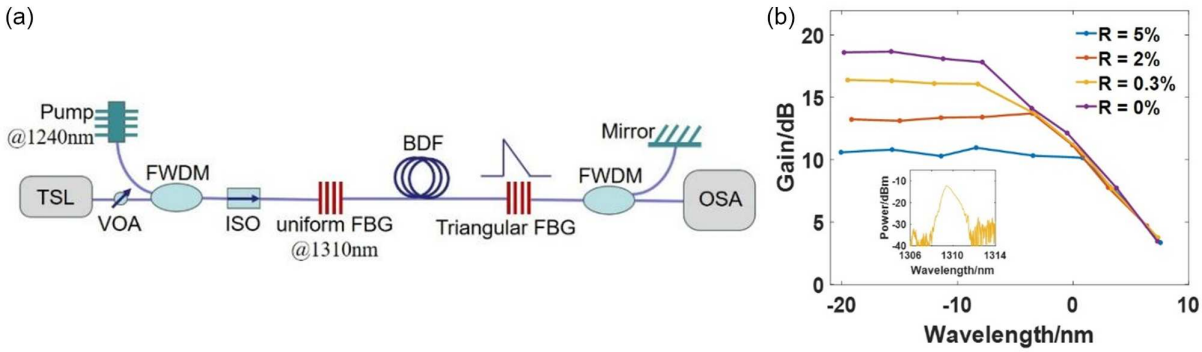

3) Tunable linear cavity for gain clamping

Based on the previous theoretical analysis, it can be known that compared with the ring cavity, the gain control efficiency of the linear cavity is higher. In 2025, Wang et al. proposed an adjustable linear cavity gain control BDFA as shown in Figure 15 [44]. Combining the broadband emission characteristics of BDFA, two circulators are used to add VOA in the linear cavity to control the cavity loss. It retains the wideband performance of the amplifier while achieving gain control. In addition, the closer to the controlled laser wavelength, the more obvious the gain suppression effect becomes. Therefore, the rational utilization of gain control can also be used for the flattening of the gain spectrum. With a pump power of 500 mW and a VOA loss of 0 dB, the gain variation of the signal less than 6 dBm is less than 0.27 dB, and the average output gain is 4.34 dB. When the VOA loss is 10 dB, the gain variation of the signal below 6 dBm is less than 0.52 dB, and the average output gain is 7.28 dB.

By comparing the gain of BDFA with adjustable linear cavity and ring cavity gain control under different VOA losses, it is easy to find that the gain curves of the two structures almost overlap without gain control, and the linear cavity has a better clamping effect when gain control is introduced. This means that the adjustable linear cavity gain control BDFA has a higher tolerance to the fluctuation of signal power under the same conditions. The complexity of the two structures presented in Figures 10 and 14 is comparable, and the reliability of the tunable line-cavity gain clamp BDFA in the transmission system is no less than that of the conventional structure.

Recently, we proposed a tunable gain-clamping structure shown in Figure 16. In this design, the linear cavity is formed with a uniform FBG and a triangular FBG. The triangular FBG used in the study was self-designed by the authors and fabricated by Shanghai Jinlei Optoelectronics Technology Co., Ltd. The triangular FBG exhibits a reflection spectrum that varies linearly with wavelength, and its reflectivity changes as the wavelength of the uniform FBG is shifted. By tuning the central wavelength of the uniform FBG via applied stress, the spectral overlap with the triangular FBG is adjusted, thereby controlling the effective reflectivity of the triangular FBG and, in turn, the intra-cavity feedback strength. In Figure16(b), R denotes the reflectivity of the triangular FBG. The results indicate that effective control of the linear cavity gain clamping can be achieved by adjusting the reflectivity of the triangular FBG.

3.4.2. Internal pump and external pump expand BDFA gain bandwidth

In 2022, Khegai et al. [57] connected phosphosilicate BDF and germanium silicate BDF in series; by applying the adjustable semi-ring semi-linear cavity, the BDFA achieved a 6 dB bandwidth of 150 nm in the O and E bands. In 2024, Wang et al. [59] constructed a two-stage BDF amplification system using 1180 nm and 1275 nm pumps. The results show that, when the input signal power was -23 dBm, a gain greater than 23 dB was achieved over the 1300–1470 nm wavelength range, with an average NF of 5 dB. In the same year, Zhai and Sahu [16] reported a dual-pump BDFA operating in the O+E+S bands. By employing dual-wavelength

Figure 17
Absorption coefficient of phosphosilicate BDF

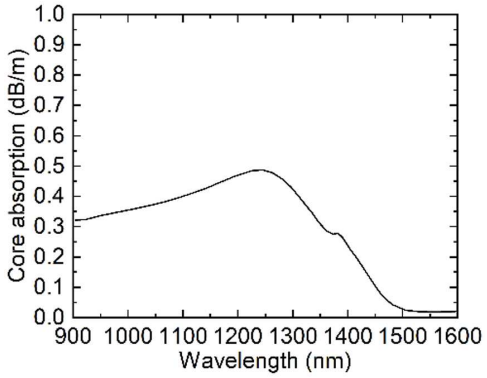

pumping at 1270 nm and 1310 nm, the amplifier achieved a 6 dB gain bandwidth of 140 nm (1333–1473 nm) under a 0 dBm input signal power.

The FORC-Photonics dataset shows the absorption coefficient of phosphosilicate BDF (refers to Figure 17). This BDF has strong absorption at both 1240 nm and 1310 nm. It is not difficult to find from Figure 11 that when the pump wavelength increases, the luminescence center of BDF shifts toward longer wavelengths. For phosphosilicate BDF, the 1240 nm and 1310 nm pumps, respectively, excite the O and E bands to emit light. If dual pumps are adopted, the gain range of the BDF can be expanded.

When considering adding a 1310 nm or longer wavelength pump to the O+E band BDFA to improve the E band gain, compared with adding a 1180 nm or other shorter wavelength pump, there is also a practical problem: it's difficult for WDM components commonly used in fiber amplifiers to separate an additional narrow channel within the signal band for the input of an O-band pump. At present, the solution to this problem mainly depends on replacing WDM with a coupler. However, this solution not only introduces higher insertion loss but also remains challenging to achieve satisfactory results. Based on this situation, we consider to replace the additional external pump with an "endogenous pump." That is, only the pump or pump combination whose wavelength is lower than the amplification range is reserved externally, such as 1240 nm or 1240+1180 nm. The pump with the required longer wavelength, such as 1310 nm, is generated through narrowband feedback, and the gain enhancement of longer wavelength is further induced by this pump. Since the endogenous pump is generated inside the amplifier, we also call it the internal pump or inner pump.

In 2024, Wang et al. [60] proposed the BDFA, adopting a linear cavity gain-clamping structure to achieve the expansion of amplification range from the O band to the O + E bands. Compared with the traditional dual-wavelength pumping, replacing the grating can achieve the wavelength transformation of the endogenous pumping. And as shown in Figure 18 [60], the 1310 nm control laser occupies less than 1 nm of bandwidth. These are convenient and cost saving for the engineering application and experimental test of BDFA. In addition, we introduce a dual-pass configuration on the basis of the line cavity; thus, high gain can be achieved with much shorter optical fibers, especially in the current situation where BDF resources are relatively precious. This design is of great significance. In particular, the requirements for the stability of the pump and the signal power of the line-cavity dual-pass BDFA are more lenient, which is conducive to its application in optical networks.

The structure proposed in Figure 14 not only enables flexible gain-clamping control but also allows regulation of the internal pump, achieving bandwidth extension without replacing the FBGs. By tuning the central wavelength of the uniform FBG via applied

Figure 18
(a) The scheme, (b) ASE, and (c) gain spectra of bandwidth-expanding dual-pass linear cavity gain control BDFA

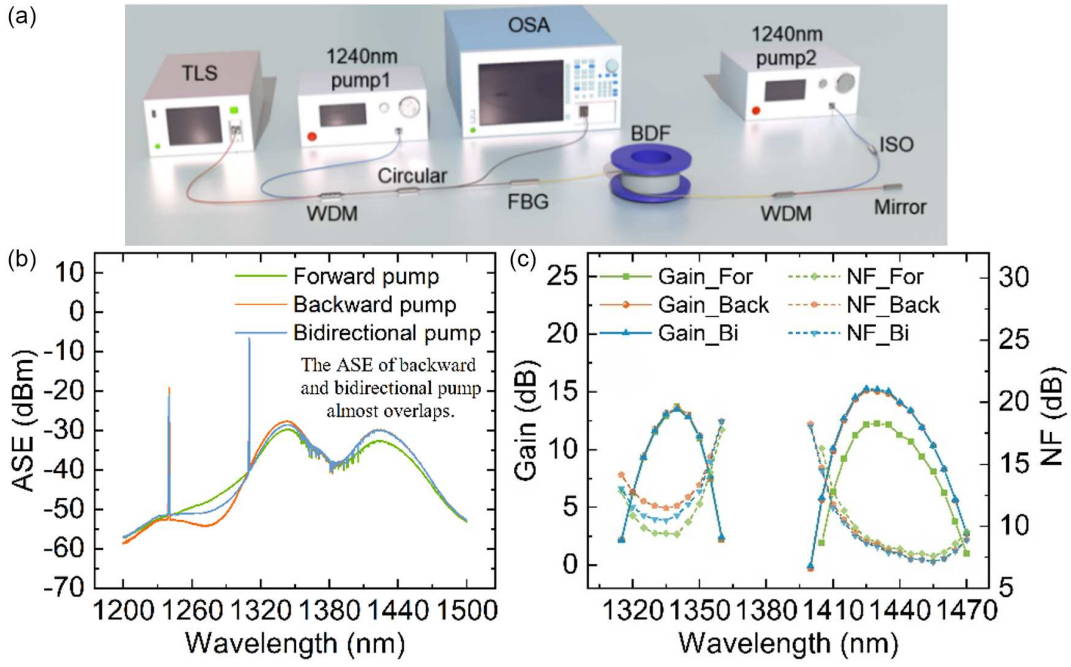

Figure 19
The bandwidth-expanding under different feedback in tunable gain-clamping linear cavity BDFA with a uniform FBG and a triangular FBG

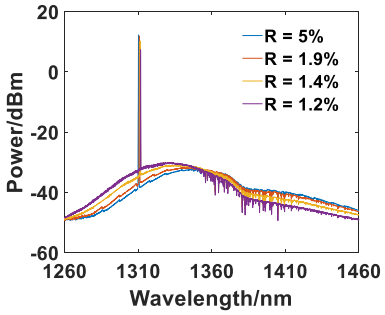

stress, the spectral overlap with the triangular FBG is adjusted, allowing precise control of intra-cavity feedback and internal pump generation, thereby extending the gain bandwidth. The ASE results shown in Figure 19 demonstrate the effectiveness of this approach. This method therefore provides a practical and efficient means to extend the gain bandwidth in BDFA systems.

4. Discussion

This paper reviews research progress in BDFA gain control technology, spanning from mature electro-optic automatic gain control to cutting-edge all-optical automatic gain control solutions. Although these techniques, particularly all-optical approaches, have demonstrated exceptional potential for gain stability and bandwidth extension in BDFAs, challenges remain in transitioning them from laboratory settings to practical applications.

First, trade-offs must be made between electrical and optical technology approaches. Electrical automatic gain control inherits the mature technology of EDFAs and offers high control precision, making it a pragmatic choice for advancing BDFA toward initial commercialization. However, its inherent electro-optic conversion and electronic delay limit response speed. All-optical automatic gain control provides rapid response, making it an ideal solution for future dynamic optical networks. Second, optimization of all-optical gain-clamping structures is essential. Traditional line-cavity and ring cavity gain control structures each possess distinct advantages. Recent work, including our proposed approach, represents a key direction for structural optimization. Future structural design should continue focusing on simplifying adjustment mechanisms, reducing insertion loss, and enhancing compatibility with BDFs.

Specifically, gain control for BDFAs cannot simply adopt the EDFA experience. BDF gain characteristics strongly depend on the type of BACs, glass matrix composition, and pump wavelength. This complexity leads to significant inhomogeneous broadening [57], potentially triggering the spectral hole burning effect and thereby causing high-gain inhomogeneity in ultra-wideband links. Gain deviation accumulation in a cascade amplifier may lead to the failure of the entire link [38]. Furthermore, the energy transfer and competition mechanisms between different BACs remain incompletely understood, complicating the development of precise gain control models. Therefore, future research must extend beyond amplifier structural innovations to deeply integrate materials science for fundamental improvements in BDF gain homogeneity.

Finally, the "endogenous pumping" approach discussed herein offers a systematic integration solution for BDFA engineering applications. It not only reduces system cost and complexity but also provides novel insights for achieving compact broadband amplification. However, this strategy relies on precise cavity feedback control, imposing higher demands on optical component performance.

5. Conclusion

The gain bandwidth coverage capability of BDFA exceeds 200 nm, far surpassing that of EDFA, which currently has relatively mature gain control technology. Due to the extremely high-gain bandwidth of BDFA and the fact that different bands are affected by different pumps to varying degrees and in different ways, this implies that the clamping effect of single-wavelength feedback may vary across different wavelength ranges. With the continuous deepening of research on ultra-wideband BDFA, clamping may also face the demand of shifting from a single wavelength to a combination of wavelengths to cover multiple bands, which also puts forward higher requirements for understanding the behavior and mechanism of BDFA under different wavelength feedbacks. On the other hand, the ultra-high-gain bandwidth characteristic of BDFA also poses higher requirements for the performance of gain-controlled devices. In the clamping structure, WDM or couplers are usually used to form a ring cavity. As the coverage bandwidth of BDFA increases, the bandwidth of such devices will affect the gain performance of BDFA and even limit its bandwidth. In comparison, FBGs have superior wideband transmission characteristics. The linear cavity structure that provides narrowband feedback using FBGs may play a more important role in the gain-clamping application of ultra-wideband BDFA. New technologies, such as BDF and space division multiplexing (SDM), not only expand the application space of traditional gain control techniques but also rely on gain-clamping techniques to provide key performance guarantees.

Funding Support

This work is sponsored by the National Key R&D Program of China (2020YFB1805802).

Ethical Statement

This study does not contain any studies with human or animal subjects performed by any of the authors.

Conflicts of Interest

The authors declare that they have no conflicts of interest to this work.

Data Availability Statement

The data that support the findings of this study are openly available in Forc-Photonics at https://www.forc-photonics.ru/en/fibers_and_cables/Bi_doped_fibers/.

Author Contribution Statement

Lihong Wang: Methodology, Formal analysis, Investigation, Writing – original draft, Visualization. **Ge Wu:** Methodology, Investigation, Writing – original draft, Visualization. **Yidan Zhao:** Validation, Investigation, Writing – review & editing. **Jingjing Zheng:** Conceptualization, Writing – original draft, Writing –

review & editing, Project administration, Funding acquisition. **Li Pei:** Resources, Supervision. **Tigang Ning:** Supervision.

References

[1] Winzer, P. J., & Neilson, D. T. (2017). From scaling disparities to integrated parallelism: A decathlon for a decade. *Journal of Lightwave Technology*, *35*(5), 1099–1115. https://doi.org/10.1109/JLT.2017.2662082

[2] Almufti, A. M., & Morozov, O. G. (2023). 1Tbit/s per lambda high order quadrature amplitude modulation (128–256QAM) coherent optical transmission system design to support (5G+). In *2023 Systems of Signal Synchronization, Generating and Processing in Telecommunications*, 1–4. https://doi.org/10.1109/SYNCHROINFO57872.2023.10178605

[3] Lowery, A. J. (2020). Spectrally efficient optical orthogonal frequency division multiplexing. *Philosophical Transactions of the Royal Society A: Mathematical, Physical and Engineering Sciences*, *378*(2169), 20190180. https://doi.org/10.1098/rsta.2019.0180

[4] Puttnam, B. J., Rademacher, G., & Luís, R. S. (2021). Space-division multiplexing for optical fiber communications. *Optica*, *8*(9), 1186–1203. https://doi.org/10.1364/OPTICA.427631

[5] Huang, C., Wang, D., Zhang, W., Wang, B., Tait, A. N., de Lima, T. F., . . . , & Prucnal, P. R. (2022). High-capacity space-division multiplexing communications with silicon photonic blind source separation. *Journal of Lightwave Technology*, *40*(6), 1617–1632. https://doi.org/10.1109/JLT.2022.3152027

[6] Sakamoto, T., Wada, M., Aozasa, S., Imada, R., Yamamoto, T., & Nakajima, K. (2021). Characteristics of randomly coupled 12-core erbium-doped fiber amplifier. *Journal of Lightwave Technology*, *39*(4), 1186–1193. https://doi.org/10.1109/JLT.2020.3047614

[7] Wang, L., Sharma, M., Maes, F., Jalilpiran, S., Durak, F. E., Messaddeq, Y., . . . , & Jiang, Z. (2022). Low cost solution for super L-band fiber amplifier based on single-mode and multi-mode hybrid pumping scheme. In *2022 Optical Fiber Communication Conference*, W3J.4. https://doi.org/10.1364/OFC.2022.W3J.4

[8] Liu, H., Wen, J., Dong, Y., Luo, Y., Wang, W., Zhang, X., . . . , & Wang, T. (2024). Bandwidth extension to 1627 nm of over 20 dB gain in an erbium-doped silica fiber via two-photon absorption. *Optics Express*, *32*(6), 8937–8949. https://doi.org/10.1364/OE.518395

[9] Chen, Y., Lou, Y., Gu, Z., Qiu, Q., He, L., Li, W., . . . , & Li, J. (2021). Extending the L-band amplification to 1623 nm using Er/Yb/P co-doped phosphosilicate fiber. *Optics Letters*, *46*(23), 5834–5837. https://doi.org/10.1364/OL.445286

[10] Jalilpiran, S., Fuertes, V., Lefebvre, J., Grégoire, N., Durak, F. E., Landry, N., . . . , & LaRochelle, S. (2023). Baria-silica erbium-doped fibers for Extended L-band amplification. *Journal of Lightwave Technology*, *41*(14), 4806–4814. https://doi.org/10.1109/JLT.2023.3244496

[11] Dianov, E. M. (2009). Bi-doped glass optical fibers: Is it a new breakthrough in laser materials? *Journal of Non-Crystalline Solids*, *355*(37–42), 1861–1864. https://doi.org/10.1016/j.jnoncrysol.2009.04.063

[12] Wen, J., Pang, F., Yang, Y., Wang, W., Liu, H., Luo, Y., & Wang, T. (2025). Chāo kuāndài guāngxiān fàngdàqì yánjiū jìnzhǎn yǔ fāzhǎn píngjǐng [Research progress and development bottleneck of ultra-wideband fiber amplifiers]. *Acta Optica Sinica*, *45*(13), 1306012. https://doi.org/10.3788/AOS250901

[13] Firstov, S. V., Alyshev, S. V., Riumkin, K. E., Khopin, V. F., Guryanov, A. N., Melkumov, M. A., & Dianov, E. M. (2016). A 23-dB bismuth-doped optical fiber amplifier for a 1700-nm band. *Scientific Reports*, *6*, 28939. https://doi.org/10.1038/srep28939

[14] Wang, Y., Thipparapu, N. K., Richardson, D. J., & Sahu, J. K. (2021). Ultra-broadband bismuth-doped fiber amplifier covering a 115-nm bandwidth in the O and E bands. *Journal of Lightwave Technology*, *39*(3), 795–800. https://doi.org/10.1109/JLT.2020.3039827

[15] Tian, J., Guo, M., Wang, F., Yu, C., Zhang, L., Wang, M., & Hu, L. (2022). High gain E-band amplification based on the low loss Bi/P co-doped silica fiber. *Chinese Optics Letters*, *20*(10), 100602. https://doi.org/10.1364/COL.20.100602

[16] Zhai, Z., & Sahu, J. K. (2024). High-gain ultra-wideband bismuth-doped fiber amplifier operating in the O + E + S band. *Optics Letters*, *49*(12), 3308–3311. https://doi.org/10.1364/OL.525583

[17] Liu, S., Yin, X., He, L., Chu, Y., Dai, N., & Li, J. (2024). High-germanium bismuth-doped fibers for U-band efficiency amplification. *Chinese Journal of Lasers*, *51*(6), 0606005. https://doi.org/10.3788/CJL231397

[18] Yang, Y., Wen, J., Wang, W., Fan, X., Dong, Y., Luo, Y., . . . , & Wang, T. (2024). Covering a 1280–1495 nm (215 nm) wideband high-gain bismuth-doped fiber amplifier with only 1240 nm pumping. *Optics Letters*, *49*(23), 6853–6856. https://doi.org/10.1364/OL.540571

[19] Taengnoi, N., Bottrill, K. R. H., Hong, Y., Wang, Y., Thipparapu, N. K., Sahu, J. K., . . . , & Richardson, D. J. (2021). Experimental characterization of an O-band bismuth-doped fiber amplifier. *Optics Express*, *29*(10), 15345–15355. https://doi.org/10.1364/OE.420995

[20] Mikhailov, V., Luo, J., Inniss, D., Yan, M. F., Sun, Y., Puc, G. S., . . . , & DiGiovanni, D. J. (2022). Amplified transmission beyond C- and L- bands: Bismuth doped fiber amplifier for O-band transmission. *Journal of Lightwave Technology*, *40*(10), 3255–3262. https://doi.org/10.1109/JLT.2022.3169172

[21] Mikhailov, V., Sun, Y., Luo, J., Khan, F., Inniss, D., Dulashko, Y., . . . , & DiGiovanni, D. J. (2024). 1255–1355 nm (17.6 THz) bandwidth O-band BDFA pumped using uncooled multimode 915 nm laser diode via YDF conversion stage. *Journal of Lightwave Technology*, *42*(4), 1265–1271. https://doi.org/10.1109/JLT.2023.3331325

[22] Firstov, S. V., Khegai, A. M., Kharakhordin, A. V., Alyshev, S. V., Firstova, E. G., Ososkov, Y. J., . . . , & Guryanov, A. N. (2020). Compact and efficient O-band bismuth-doped phosphosilicate fiber amplifier for fiber-optic communications. *Scientific Reports*, *10*(1), 11347. https://doi.org/10.1038/s41598-020-68243-4

[23] Firstov, S., Khegai, A., Riumkin, K., Ososkov, Y., Firstova, E., Melkumov, M., . . . , & Guryanov, A. (2020). Bend-insensitive bismuth-doped P2O5-SiO2 glass core fiber for a compact O-band amplifier. *Optics Letters*, *45*(9), 2576–2579. https://doi.org/10.1364/OL.389117

[24] Donodin, A., Dvoyrin, V., Manuylovich, E., Krzczanowicz, L., Forysiak, W., Melkumov, M., . . . , & Turitsyn, S. (2021). Bismuth doped fibre amplifier operating in E- and S- optical bands. *Optical Materials Express*, *11*(1), 127–135. https://doi.org/10.1364/OME.411466

[25] Zhai, Z., Halder, A., & Sahu, J. K. (2024). High gain bismuth-doped fiber amplifier operating in the E+S band with record gain per unit length. *Journal of Lightwave Technology*, *42*(15), 5375–5382. https://doi.org/10.1109/JLT.2024.3417823

[26] Liu, S. K., Yin, X. K., He, L., Li, W. Z., Chu, Y. B., Dai, N. L., & Li, J. Y. (2025). Realizing 48.5 dB gain in the E+S band using 12 m bismuth-doped fiber. *Advanced Optical Materials*, *13*(3), 2401798. https://doi.org/10.1002/adom.202401798

[27] Wan, H., Qi, J., Liao, Z., Zhou, S., Huang, X., Chu, J., . . . , & Luo, J. (2024). S-band fiber amplifier with exceed 28 dB gain across 1460 ~1530 nm. In *2024 Asia Communications and Photonics Conference and International Conference on Information Photonics and Optical Communications*, 1–4. https://doi.org/10.1109/acp/ipoc63121.2024.10809923

[28] Li, X., Tian, J., Shao, C., Guo, M., Chen, Y., Yu, C., & Hu, L. (2025). Ultra-broadband emission in Bi/Ge co-doped silica glass and fiber via bismuth coordination engineering. *Advanced Optical Materials*, *13*(4), 2402261. https://doi.org/10.1002/adom.202402261

[29] Wang, Y., Wang, S., Halder, A., & Sahu, J. K. (2023). (Invited) Bi-doped optical fibers and fiber amplifiers. *Optical Materials: X*, *17*, 100219. https://doi.org/10.1016/j.omx.2022.100219

[30] Song, K., & Lauder, R. D. T. (1999). An analytical formulation of the transient response of gain-clamped EDFA's. *IEEE Photonics Technology Letters*, *11*(11), 1378–1380. https://doi.org/10.1109/68.803051

[31] Ellis, A. D., Percival, R. M., Lord, A., & Stallard, W. A. (1991). Automatic gain control in cascaded erbium doped fibre amplifier systems. *Electronics Letters*, *27*(3), 193–195. https://doi.org/10.1049/el:19910125

[32] Na, K.-W., Choi, J.-T., Lee, W.-J., Park, S.-H., Yoon, W.-W., & Lee, K.-K. (2000). A cost-effective gain control using pump modulation for erbium-doped fiber amplifiers. *IEEE Photonics Technology Letters*, *12*(4), 383–385. https://doi.org/10.1109/68.839026

[33] Massicott, J. F., Willson, S. D., Wyatt, R., Armitage, J. R., Kashyap, R., Williams, D., & Lobbett, R. A. (1994). 1480 nm pumped erbium doped fibre amplifier with all optical automatic gain control. *Electronics Letters*, *30*(12), 962–964. https://doi.org/10.1049/el:19940660

[34] Yi, L., Zhan, L., Hu, W., Tang, Q., & Xia, Y. (2006). Tunable gain-clamped double-pass Erbium-doped fiber amplifier. *Optics Express*, *14*(2), 570–574. https://doi.org/10.1364/OPEX.14.000570

[35] Ji, J. H., Zhan, L., Yi, L. L., Tang, C. C., Ye, Q. H., & Xia, Y. X. (2005). Low noise-figure gain-clamped L-band double-pass erbium-doped fiber ring lasing amplifier with an interleaver. *Journal of Lightwave Technology*, *23*(3), 1375–1379. https://doi.org/10.1109/JLT.2004.841441

[36] Mahdi, M. A., Mahamd Adikan, F. R., Subramaniam, T., & Ahmad, H. (2007). Characterization of lasing-oscillation direction in optical gain-clamped erbium-doped fiber amplifiers. *Optics & Laser Technology*, *39*(5), 1020–1024. https://doi.org/10.1016/j.optlastec.2006.05.006

[37] Oikawa, Y., Sato, N., Ota, K., Petit, S., & Shiga, N. (2012). 0.2-dB gain excursion AGC-EDFA with a high speed VOA for 100-channel add/drop equivalent operation. In *2012 Optical Fiber Communication Conference, OW4D.3*. https://doi.org/10.1364/OFC.2012.OW4D.3

[38] Wang, L., Fung, Y., Sharma, M., Botzung, C., LaRochelle, S., & Jiang, Z. (2023). Bandwidth-dependent gain deviation in E+S band bismuth doped fiber amplifier under automatic gain control. In *2023 Optical Fiber Communication Conference, Th3C.3*. https://doi.org/10.1364/OFC.2023.Th3C.3

[39] Cai, M., Liu, X., Cui, J., Tang, P., & Peng, J. (1997). Study on noise characteristic of gain-clamped erbium-doped fiber-ring lasing amplifier. *IEEE Photonics Technology Letters*, *9*(8), 1093–1095. https://doi.org/10.1109/68.605511

[40] Bononi, A., & Barbieri, L. (1999). Design of gain-clamped doped-fiber amplifiers for optimal dynamic performance. *Journal of Lightwave Technology*, *17*(7), 1229–1240. https://doi.org/10.1109/50.774262

[41] Durak, F. E., & Altuncu, A. (2017). Gain clamped l-band EDFA based on a lasing structure using FBG. In *2017 Advances in Wireless and Optical Communications*, 24–27. https://doi.org/10.1109/RTUWO.2017.8228498

[42] Yu, A., & Mahony, M. J. O. (1997). Design and modeling of laser-controlled erbium-doped fiber amplifiers. *IEEE Journal of Selected Topics in Quantum Electronics*, *3*(4), 1013–1018. https://doi.org/10.1109/2944.649531

[43] Jiang, C. (2009). Modeling a broadband bismuth-doped fiber amplifier. *IEEE Journal on Selected Topics in Quantum Electronics*, *15*(1), 79–84. https://doi.org/10.1109/JSTQE.2008.2010269

[44] Wang, L., Ning, T., Pei, L., Zheng, J., Xu, W., Wang, J., & Li, J. (2025). Tunable gain-clamped linear cavity bismuth-doped fiber amplifier operating in the O-band. *Journal of Lightwave Technology*, *43*(7), 3472–3478. https://doi.org/10.1109/JLT.2024.3512513

[45] Luo, G., Zyskind, J. L., Nagel, J. A., & Ali, M. A. (1998). Experimental and theoretical analysis of relaxation-oscillations and spectral hole burning effects in all-optical gain-clamped EDFA's for WDM networks. *Journal of Lightwave Technology*, *16*(4), 527–533. https://doi.org/10.1109/50.664059

[46] Zhao, C.-L., Tam, H.-Y., Guan, B.-O., Dong, X., Wai, P. K. A., & Dong, X. (2003). Optical automatic gain control of EDFA using two oscillating lasers in a single feedback loop. *Optics Communications*, *225*(1–3), 157–162. https://doi.org/10.1016/j.optcom.2003.07.020

[47] Lin, M., Mo, J., Lao, H., & Dong, X. (2022). Three-stage gain-clamped L-band EDFA with low noise-figure base on ring lasing. In *2022 20th International Conference on Optical Communications and Networks*, 1–2. https://doi.org/10.1109/icocn55511.2022.9901131

[48] Wu, Z., Lao, H., Zou, Y., Gao, Z., Xu, P., & Dong, X. (2023). Dual-stage gain-clamped L-band extended EYDFA with a ring cavity laser. In *2023 21st International Conference on Optical Communications and Networks*, 1–3. https://doi.org/10.1109/icocn59242.2023.10236316

[49] Inoue, K. (1999). Gain-clamped fiber amplifier with a short length of preamplification fiber. *IEEE Photonics Technology Letters*, *11*(9), 1108–1110. https://doi.org/10.1109/68.784203

[50] Yang, J., Meng, X., & Liu, C. (2016). Accurately control and flatten gain spectrum of L-band erbium doped fiber amplifier based on suitable gain-clamping. *Optics & Laser Technology*, *78*, 74–78. https://doi.org/10.1016/j.optlastec.2015.10.019

[51] Durak, F. E., & Altuncu, A. (2018). All-optical gain clamping and flattening in L-Band EDFAs using lasing-controlled structure with FBG. *Optical Fiber Technology*, *45*, 217–222. https://doi.org/10.1016/j.yofte.2018.07.014

[52] Yang, J., & Liu, C. (2016). Simultaneously flatten and clamp gain spectrum of L-band EDFA by accurate FBG-based gain-control. In *2016 Asia Communications and*

Photonics Conference, 1–2. https://doi.org/10.1364/ACPC.2016.AF2A.120

[53] Yang, J., & Liu, C. (2017). Multi-wavelength L-band gain-clamped erbium-doped fiber amplifier with high gain and flatness by using composite FBGS. *Microwave and Optical Technology Letters*, *59*(3), 691–695. https://doi.org/10.1002/mop.30376

[54] Zhang, S., Dong, Y. H., Zhang, J. N., Zhang, X. B., Wang, T. Y., & Guo, Y. (2024). An erbium-doped fiber amplifier with tunable gain-clamping in the extended L-band. *IEEE Photonics Technology Letters*, *36*(9), 617–620. https://doi.org/10.1109/LPT.2024.3384707

[55] Wada, M., Aozasa, S., Sakamoto, T., Mori, T., Yamamoto, T., & Nakajima, K. (2018). Gain-clamped 4-LP-mode erbium-doped fiber amplifier with low temporal gain variation. *Journal of Lightwave Technology*, *36*(5), 1233–1238. https://doi.org/10.1109/JLT.2018.2799549

[56] Ono, H., & Yamada, M. (2023). Static analysis of gain control for a few-mode erbium-doped fiber amplifier employing pump power adjustment. *Applied Optics*, *62*(16), 4180–4186. https://doi.org/10.1364/AO.488413

[57] Khegai, A., Ososkov, Y., Firstov, S., Riumkin, K., Alyshev, S., Kharakhordin, A., . . . , & Melkumov, M. (2022). Gain clamped Bi-doped fiber amplifier with 150 nm bandwidth for O- and E-bands. *Journal of Lightwave Technology*, *40*(4), 1161–1166. https://doi.org/10.1109/JLT.2021.3127945

[58] Wang, D., Pei, L., Zheng, J., Wang, J., Hou, W., Zhang, F., . . . , & Li, J. (2024). Comparative experimental study on gain clamping performance of O-band BDFA with different pump schemes at different input powers. *Optics & Laser Technology*, *171*, 110340. https://doi.org/10.1016/j.optlastec.2023.110340

[59] Wang, W., Yang, Y., Wen, J., Dong, Y., Luo, Y., Fan, X., . . . , & Wang, T. (2024). Ultra-broadband bismuth-doped fiber amplifier with 170 nm bandwidth using a two-stage configuration. *Optics Letters*, *49*(24), 7242–7245. https://doi.org/10.1364/OL.541546

[60] Wang, L., Ning, T., Pei, L., Zheng, J., Ye, X., Zhang, F., . . . , & Li, J. (2024). Bismuth-doped fiber amplifier based on a linear cavity double pass structure operating in the O + E band. *Optics Express*, *32*(12), 21007–21016. https://doi.org/10.1364/OE.525101

How to Cite: Wang, L., Wu, G., Zhao, Y., Zheng, J., Pei, L., & Ning, T. (2026). Advances in Gain Control Techniques for Bismuth-Doped Fiber Amplifier. *Journal of Optics and Photonics Research*. https://doi.org/10.47852/bonviewJOPR62027286